Am J Transl Res 2026;18(1):112-123
www.ajtr.org /ISSN:1943-8141/AJTR0165235

Original Article

Construction and validation of a predictive model for intraoperative rupture risk in microscopic surgical clipping of intracranial aneurysms

Jun Zhang[1], Yuan Wang[2], Yanbin Liang[3], Tao Huang[3], Jingku Ma[4]

[1]*Department of Neurosurgery, Hanzhong Central Hospital, No. 557, Middle Section of Laodong West Road, Hantai District, Hanzhong 723000, Shaanxi, China;* [2]*Department of Oncology, 3201 Hospital, No. 783 Tianhan Avenue, Hanzhong 723000, Shaanxi, China;* [3]*Department of Neurosurgery, 3201 Hospital, No. 783 Tianhan Avenue, Hanzhong 723000, Shaanxi, China;* [4]*Department of Neuro Intensive Care Unit, No. 215 Hospital of Shaanxi Nuclear Industry, No. 52 Weiyang West Road, Qindu District, Xianyang 712000, Shaanxi, China*

Received April 10, 2025; Accepted August 23, 2025; Epub January 15, 2026; Published January 30, 2026

Abstract: Objectives: To identify risk factors for intraoperative rupture during microscopic clipping of intracranial aneurysms (IA) and to develop a predictive nomogram for improved preoperative risk assessment and surgical outcomes. Methods: A retrospective analysis was conducted on 286 IA patients who underwent surgical clipping between January 2018 and January 2023. Patients were classified into rupture (n=56) and non-rupture (n=230) groups based on intraoperative outcomes. Clinical data, including demographics, aneurysm size, morphology, and preoperative functional status, were collected. Independent risk factors were identified using multivariate logistic regression, and a nomogram model was constructed. Model performance was evaluated by ROC curves, calibration plots, and decision curve analysis (DCA). Six-month postoperative outcomes and complication rates were compared between the groups. Results: Univariate analysis showed that age ≥60 years, cerebral vasospasm, aneurysm diameter ≥10 mm, irregular morphology, anterior communicating artery location, preoperative Hunt-Hess grade >III, and the use of adjunctive techniques were associated with increased rupture risk. Multivariate regression identified cerebral vasospasm (OR=2.387, P=0.012), aneurysm size ≥10 mm (OR=2.298, P=0.018), anterior communicating artery aneurysm (OR=2.800, P=0.004), Hunt-Hess grade >III (OR=2.625, P=0.006), and adjunctive techniques (OR=2.492, P=0.012) as independent predictors. Interestingly, irregular morphology emerged as a protective factor (OR=0.348, P=0.003). The nomogram achieved an AUC of 0.856 in the training cohort and 0.763 in the validation cohort (P=0.438). Calibration curves demonstrated strong agreement between predicted and observed outcomes, while DCA indicated clinical benefit at threshold probabilities of 0-41%. At six months, patients in the rupture group had significantly worse modified Rankin Scale scores and higher complication rates (P<0.05). Conclusion: The proposed nomogram provides a reliable tool for predicting intraoperative rupture during IA clipping, enabling individualized preoperative risk assessment and optimization of surgical strategies, particularly in high-risk patients.

Keywords: Intracranial aneurysm, intraoperative rupture, microscopic surgical clipping, logistic regression, nomogram, risk prediction

Introduction

Intracranial aneurysm (IA) is a critical cerebrovascular disorder characterized by abnormal dilatation of the arterial wall. The reported prevalence ranges from 0.2% to 7.9% across populations, with high mortality and morbidity rates [1, 2]. Rupture typically presents as sudden subarachnoid hemorrhage (SAH), which carries a substantial risk of death. Studies indicate that mortality after first rupture may reach 43%, with most deaths occurring within 24 hours [3-5], underscoring the importance of prevention and treatment in neurosurgical practice.

The pathogenesis of IA is multifactorial, involving both congenital and acquired mechanisms. Congenital theories emphasize developmental arterial wall defects, particularly at Circle of Willis bifurcations, as key drivers of aneurysm formation [6]. Acquired mechanisms focus on

https://doi.org/10.62347/GASI9571

degenerative vascular changes, such as atherosclerosis and hypertension-induced damage to the internal elastic lamina [7]. Trauma and infection may also contribute. Clinically, IA presentations vary: approximately 50% of patients present with SAH, while others develop neurological deficits due to mass effect or are diagnosed incidentally during imaging [8].

Previous studies have identified several risk factors for intraoperative rupture during microscopic clipping, including patient demographics, aneurysm size, morphology, anatomical location, and intraoperative conditions [9]. However, few comprehensive predictive models integrating these factors are available for clinical decision-making.

Current IA treatment includes microsurgical clipping and endovascular therapy, particularly coil embolization [10]. Since the introduction of detachable coils in the 1990s, endovascular approaches have gained widespread adoption due to their minimally invasive nature and favorable outcomes [11]. The landmark ISAT trial demonstrated a 22.6% relative risk reduction in poor outcomes with endovascular therapy compared to surgical clipping, with significantly lower mortality and morbidity [12]. Nonetheless, endovascular procedures carry inherent risks, with intraoperative rupture reported in 2.8-7.7% of cases, often leading to poor prognosis [13].

Microsurgical clipping remains a cornerstone treatment, especially for complex aneurysms, because of its high occlusion rates and low recurrence [14]. Emergency microsurgical intervention also plays a vital role in ruptured aneurysms requiring immediate management. However, the significant risk of intraoperative rupture necessitates systematic investigation of predictive factors and development of reliable risk assessment tools.

Therefore, this study aimed to identify risk factors for intraoperative rupture during microscopic clipping of IA and to construct a predictive nomogram to improve preoperative evaluation and surgical planning.

Methods and materials

Sample size

Based on the study by Sharma et al. [15], the incidence of intraoperative rupture in patients with IA is 12.1%. Using the formula $N = Z^2 \times [P \times (1-P)]/E^2$, where Z=1.96, P=0.121, and E=0.05, the required sample size was calculated as 162.

Sample source

A retrospective analysis was performed on 286 IA patients who underwent microscopic surgical clipping at Hanzhong Central Hospital, 3201 Hospital, and No. 215 Hospital of Shaanxi Nuclear Industry between January 2018 and January 2023. Patients experiencing intraoperative rupture and hemorrhage were assigned to the rupture group (n=56), while those without rupture were assigned to the non-rupture group (n=230). This study was approved by the Ethics Committee of No. 215 Hospital of Shaanxi Nuclear Industry.

Inclusion and exclusion criteria

Inclusion criteria: (1) Age >18 years. (2) Patients who underwent microscopic clipping at the above three hospitals between January 2018 and January 2023. (3) Diagnosis of IA confirmed by imaging. (4) Complete clinical data, including preoperative, intraoperative, and postoperative follow-up information. (5) Clear surgical records documenting intraoperative rupture and hemorrhage.

Exclusion criteria: (1) Severe systemic diseases (e.g., advanced malignancy). (2) Missing imaging or intraoperative records. (3) Incomplete surgeries (terminated intraoperatively). (4) Unclear intraoperative rupture status.

Clinical data collection

Collected variables included demographics (age, sex), medical history (hypertension, diabetes, smoking, alcohol use), and preoperative functional status assessed by the Hunt-Hess grade. Imaging data from computed tomography angiography, magnetic resonance angiography, or digital subtraction angiography were used to evaluate aneurysm size (mm), morphology (saccular or fusiform; regular or irregular), and location (e.g., anterior communicating artery, middle cerebral artery). Intraoperative data included timing, site of rupture, and surgical management. Postoperative follow-up included modified Rankin Scale (mRS) scores at six months and complications such as re-rupture, infection, or neurological deficits.

Detection methods

Aneurysm size was categorized as ≥10 mm or <10 mm. Morphology was independently classified as regular or irregular by two experienced neurosurgeons. Preoperative functional status was graded using Hunt-Hess, and six-month outcomes were assessed by mRS, with scores 0-2 defined as good prognosis and >2 as poor prognosis [16, 17].

Training and validation groups

Patients were randomly divided into a training cohort (n=188) and a validation cohort (n=98) in a 67%:33% ratio. Stratification was balanced according to six variables: cerebral vasospasm (yes/no), aneurysm size (≥10 mm/<10 mm), morphology (regular/irregular), anterior communicating artery location (yes/no), Hunt-Hess grade (>III/≤III), and use of adjunctive techniques (yes/no). Chi-square tests confirmed no significant baseline differences between the groups. An additional 91 patients treated at the same hospitals from January 2018 to December 2019 were included as an external validation cohort. Adjunctive techniques included (1) intraoperative indocyanine green fluorescence angiography for real-time assessment of vessel patency, and (2) intraoperative Doppler ultrasonography for dynamic monitoring of blood flow during aneurysm manipulation and clipping.

Outcome measures

The primary outcome was intraoperative aneurysm rupture. Secondary outcomes included comparisons of baseline characteristics between rupture and non-rupture groups, six-month mRS scores, complication rates, and identification of risk factors for intraoperative rupture.

Statistical analysis

Statistical analyses were performed using SPSS 25.0 and R 4.3.3. Categorical variables expressed as counts and rates were compared by chi-square test. Logistic regression was used to identify independent risk factors. A predictive nomogram was constructed in R based on regression results. Model discrimination was evaluated with ROC curves, calibration was assessed by calibration plots, and clinical utility was examined using decision curve analysis (DCA). DeLong's test was applied to compare AUCs between training and validation cohorts. A *P*-value <0.05 was considered statistically significant.

Results

Comparison of basic information between non-rupture and rupture groups

As shown in **Table 1**, patients aged ≥60 years were significantly more common in the rupture group (P=0.003). Cerebrovascular stenosis, including both proximal and distal segments, was also more frequent in the rupture group (P< 0.001). The incidence of cerebral vasospasm was significantly higher (P=0.001), and aneurysms with maximum diameter ≥10 mm were more prevalent in the rupture group (P=0.002). Anterior communicating artery aneurysms were more frequent (P=0.004), as were cases with a preoperative Hunt-Hess grade >III (P=0.002). The use of adjunctive techniques was significantly higher in the rupture group (P<0.001). In contrast, no significant differences were observed between groups in sex (P=0.564), body mass index (P=0.431), diabetes (P=0.606), hypertension (P=0.757), smoking (P=0.696), alcohol consumption (P=0.349), or modified Fisher grade >II (P=0.665).

Univariate logistic regression analysis

Before logistic regression, Pearson correlation and variance inflation factor (VIF) analysis were performed to assess collinearity. Correlation coefficients were <0.3 and all VIF values <5, indicating no significant multicollinearity (Table S1; **Figure 1**). Univariate logistic regression identified several risk factors significantly associated with intraoperative rupture: age ≥60 years (OR=2.468, 95% CI: 1.359-4.591, P= 0.003), cerebral vasospasm (OR=2.614, 95% CI: 1.446-4.773, P=0.002), aneurysm diameter ≥10 mm (OR=2.500, 95% CI: 1.385-4.570, P=0.003), anterior communicating artery location (OR=2.392, 95% CI: 1.300-4.381, P= 0.005), Hunt-Hess grade >III (OR=2.500, 95% CI: 1.380-4.623, P=0.003), and use of adjunctive techniques (OR=3.673, 95% CI: 1.947-6.916, P<0.001). Conversely, cerebrovascular stenosis (OR=0.460, 95% CI: 0.266-0.799, P= 0.005) and regular aneurysm morphology (OR= 0.405, 95% CI: 0.214-0.742, P=0.004) were

Table 1. Comparison of baseline data between non-rupture and rupture groups

Factor	Non-Rupture Group (n=230)	Rupture Group (n=56)	Statistic Value	*P*-value
Age			8.851	0.003
≥60	97 (42.17%)	36 (64.29%)		
<60	133 (57.83%)	20 (35.71%)		
Gender			0.333	0.564
Male	133 (57.83%)	30 (53.57%)		
Female	97 (42.17%)	26 (46.43%)		
Body Mass Index			1.684	0.431
18-21.9	74 (32.17%)	20 (35.71%)		
22-24.9	110 (47.83%)	29 (51.79%)		
≥25	46 (20%)	7 (12.50%)		
History of Diabetes			0.265	0.606
Yes	35 (15.22%)	7 (12.50%)		
No	195 (84.78%)	49 (87.50%)		
History of Hypertension			0.096	0.757
Yes	53 (23.04%)	14 (25.00%)		
No	177 (76.96%)	42 (75.00%)		
History of Smoking			0.152	0.696
Yes	138 (60.00%)	32 (57.14%)		
No	92 (40.00%)	24 (42.86%)		
History of Alcohol Consumption			0.878	0.349
Yes	87 (37.83%)	25 (44.64%)		
No	143 (62.17%)	31 (55.36%)		
Cerebral Vasculature Stenosis			8.843	0.012
No	207 (90.00%)	43 (76.79%)		
Near-end	18 (7.83%)	8 (14.28%)		
Far-end	5 (2.17%)	5 (8.93%)		
Cerebral Vasospasm			10.417	0.001
Yes	74 (32.17%)	31 (55.36%)		
No	156 (67.83%)	25 (44.64%)		
Maximum Aneurysm Diameter			9.451	0.002
≥10 mm	80 (34.78%)	32 (57.14%)		
<10 mm	150 (65.22%)	24 (42.86%)		
Regular Morphology			8.538	0.003
Yes	124 (53.91%)	18 (32.14%)		
No	106 (46.09%)	38 (67.86%)		
Anterior Communicating Artery Aneurysm			8.25	0.004
Yes	58 (25.22%)	25 (44.64%)		
No	172 (74.78%)	31 (55.36%)		
Preoperative Hunt-Hess Grade			9.235	0.002
>III	92 (40.00%)	35 (62.50%)		
≤III	138 (60.00%)	21 (37.50%)		
Modified Fisher Grade			0.188	0.665
>II	81 (35.22%)	18 (32.14%)		
≤II	149 (64.78%)	38 (67.86%)		
Use of Adjunctive Techniques			17.59	<0.001
Yes	39 (16.96%)	24 (42.86%)		
No	191 (83.04%)	32 (57.14%)		

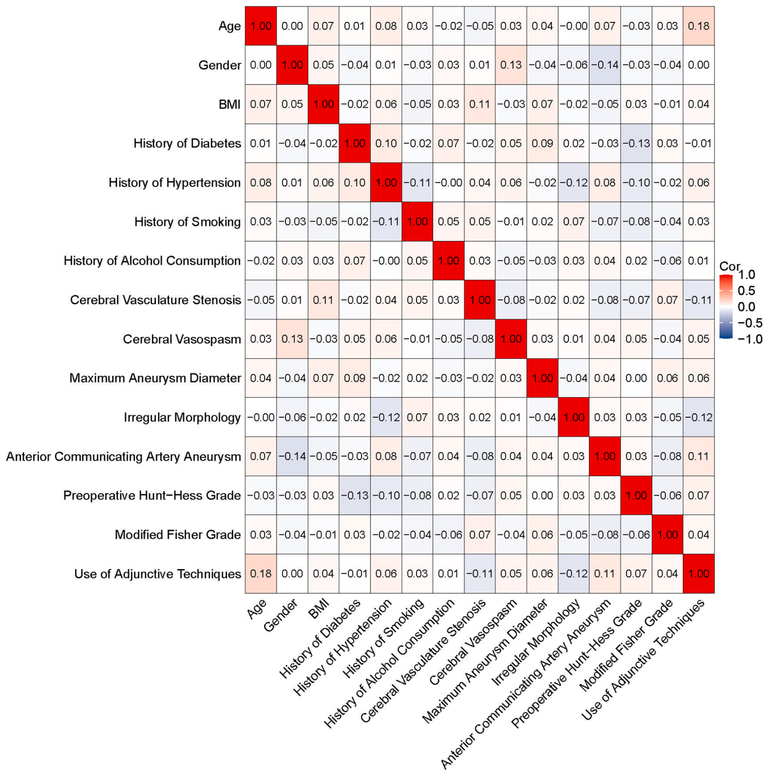

Figure 1. Correlation analysis determines the linear relationship between the variables. Note: BMI, body mass index.

associated with a lower risk of rupture (**Figure 2A**).

Multivariate logistic regression analysis identified independent predictors of intraoperative rupture. Cerebral vasospasm (OR=2.387, 95% CI: 1.218-4.730, P=0.012), aneurysm diameter ≥10 mm (OR=2.298, 95% CI: 1.160-4.615, P=0.018), anterior communicating artery location (OR=2.800, 95% CI: 1.381-5.744, P=0.004), Hunt-Hess grade >III (OR=2.625, 95% CI: 1.341-5.278, P=0.006), and use of adjunctive techniques (OR=2.492, 95% CI: 1.211-5.091, P=0.012) all increased rupture risk. In contrast, regular aneurysm morphology served as an independent protective factor (OR=0.348, 95% CI: 0.168-0.695, P=0.003) (**Figure 2B**).

Nomogram model and validation. A nomogram was constructed based on multivariate logistic regression results (**Figure 3**), incorporating cerebral vasospasm, aneurysm diameter, morphology, anterior communicating artery location, preoperative Hunt-Hess grade, and use of adjunctive techniques. ROC curve analysis (**Figure 4**) showed that the nomogram had an AUC of 0.824, significantly outperforming any single predictor (P<0.001), demonstrating strong discriminative ability.

Comparison of predictive ability between training and validation groups after model splitting

To assess the stability and predictive performance of the nomogram, the dataset was randomly divided into training and validation cohorts at a 67%:33% ratio. Baseline characteristics, including rupture status, cerebral vasospasm, aneurysm size, morphology, anterior communicating artery location, preoperative Hunt-Hess grade, and use of adjunctive techniques, showed no significant differences between the two groups (all P>0.05), ensuring comparability. Additionally, an external validation cohort of 91 patients was analyzed, and no significant baseline differences were observed compared with either the training or validation group (all P>0.05), confirming the robustness of the model across different cohorts (**Table 2**).

ROC curve analysis demonstrated good discriminative performance, with AUC values of 0.824 in the training cohort and 0.763 in the validation cohort (**Figure 5A**, **5B**). DeLong's test revealed no significant difference between the two groups (D=0.777, P=0.438), indicating consistent predictive capability. The external validation cohort achieved an AUC of 0.792 (**Figure 5C**), further supporting the model's generalizability.

Calibration curve analysis showed strong agreement between predicted probabilities and actual outcomes. In the training cohort (**Figure 6A**), both the apparent and bias-corrected calibration curves closely aligned with the ideal reference line. In the validation cohort (**Figure 6B**), slight deviation was observed at higher predicted probabilities, but overall calibration remained satisfactory, with both curves falling within the 95% confidence interval. The

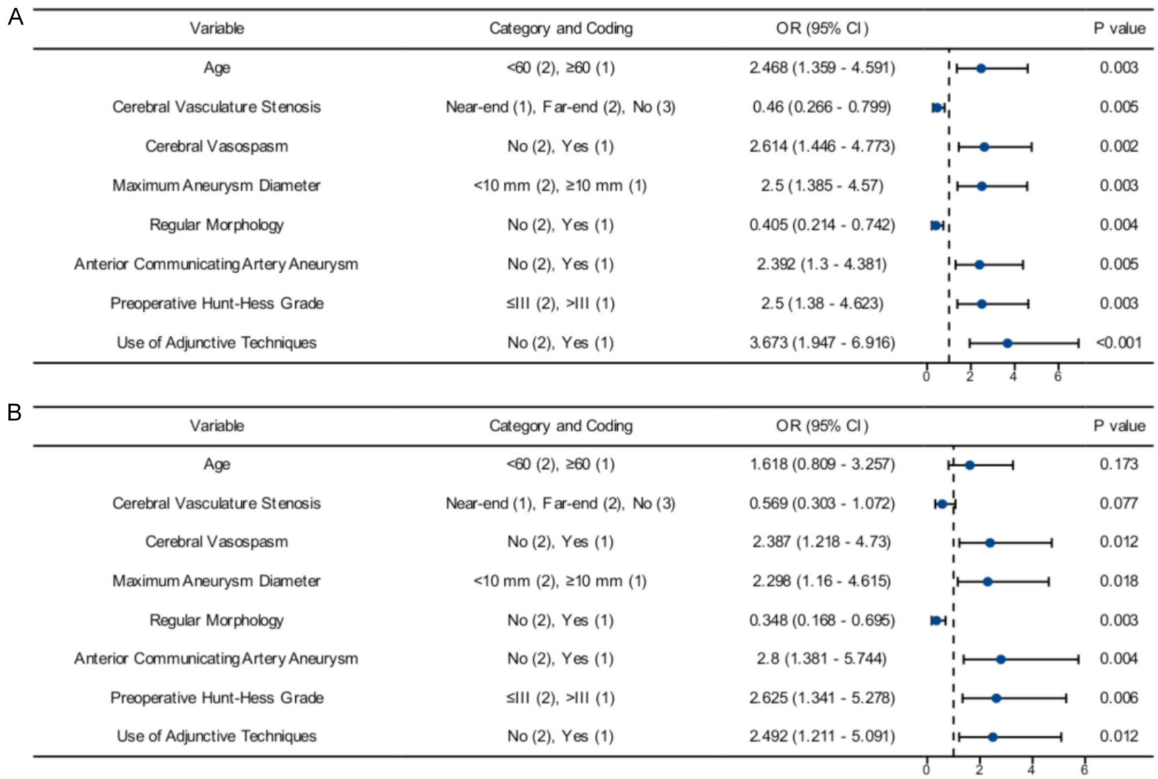

Figure 2. logistics regression analysis of risk factors for rupture bleeding during aneurysm. A. Univariate logistic regression analysis of factors associated with rupture bleeding during aneurysm surgery. B. Multivariate logistic regression analysis of factors associated with rupture bleeding during aneurysm surgery.

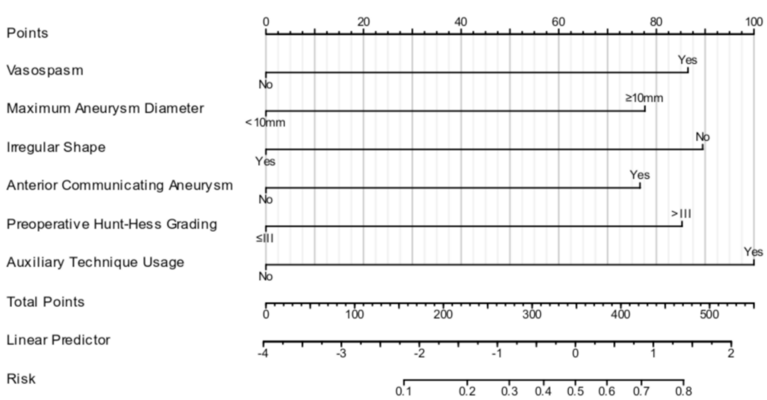

Figure 3. Nomogram model for predicting IA rupture and hemorrhage. Note: IA, intracranial aneurysm.

external validation cohort also demonstrated good calibration (**Figure 6C**), reinforcing the model's reliability.

DCA demonstrated that the nomogram provided clinical net benefit across a wide range of threshold probabilities (0-78%). The maximum net benefit was 20.21% in the training cohort, 18.36% in the validation cohort, and 17.58% in the external validation cohort (**Figure 7A-C**), confirming its clinical utility.

Six-month postoperative prognosis and complications

At six months, functional outcomes differed significantly between the groups. In the non-rupture cohort, 207 patients achieved favorable outcomes (mRS 0-2), while 23 had poor outcomes (mRS >2). In the rupture cohort, only 39 patients had favorable outcomes, and 17 had poor outcomes, demonstrating significantly worse functional recovery compared with the non-rupture cohort (P<0.001; **Figure 8A**).

Complication rates were also higher in the rupture cohort: 10 patients experienced complications compared with 15 in the non-rupture cohort, despite the smaller sample size of the rupture group. The difference in complication

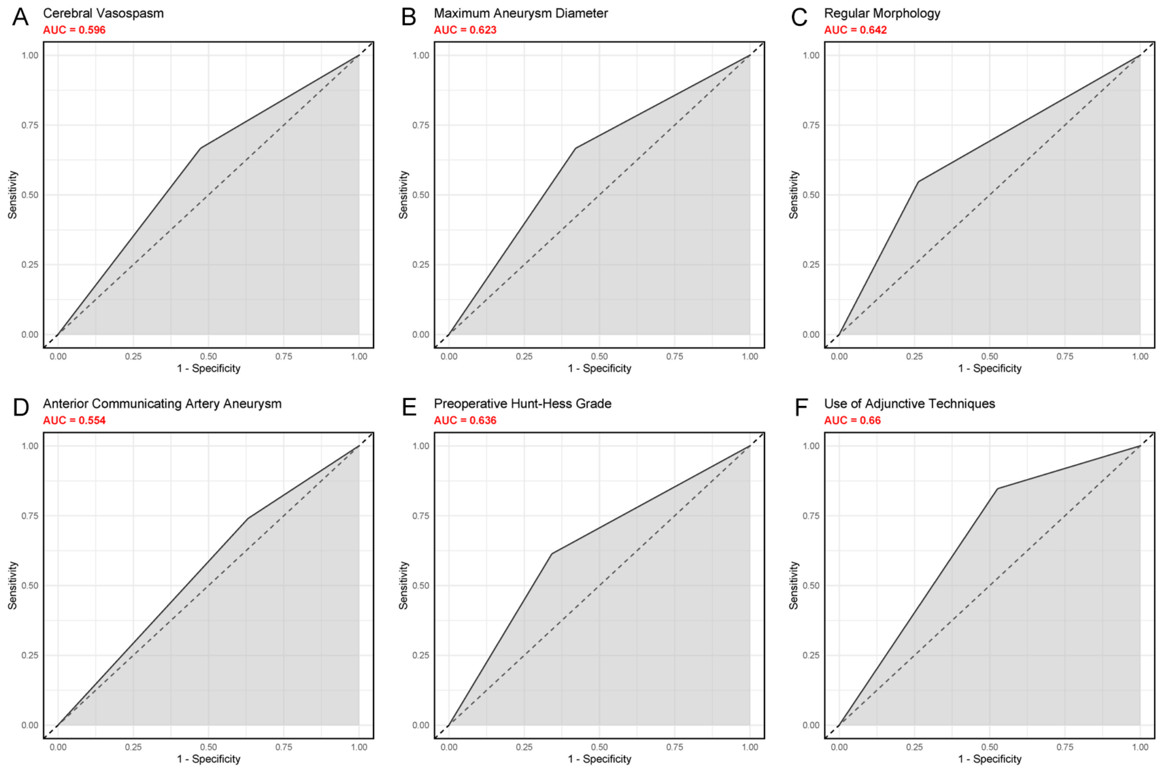

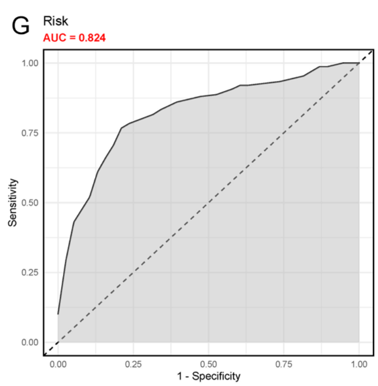

Figure 4. ROC curve of prediction model and single variable for predicting intraoperative hemorrhage from aneurysm rupture in patients. A. ROC curve of carotid artery spasm for predicting intraoperative hemorrhage from aneurysm rupture in patients. B. ROC curve of the maximum diameter of aneurysm predicting intraoperative rupture and bleeding in patients with aneurysm. C. ROC curve of rule form to predict intraoperative rupture bleeding of patient's aneurysm. D. ROC curve for predicting intraoperative hemorrhage in patients with previous traffic artery aneurysm. E. ROC curve for predicting intraoperative hemorrhage in patients with Hunt-Hess grade before surgery. F. ROC curve for predicting intraoperative hemorrhage in patients with auxiliary technology use. G. ROC curve for predicting intraoperative hemorrhage in patients with risk prediction model. Note: ROC, Receiver Operating Characteristic; AUC, Area Under the Curve.

incidence between the two groups was statistically significant (P=0.014; **Figure 8B**).

Discussion

IA is a critical condition that may progress to cerebrovascular complications and neurological damage, with rupture leading to SAH. Microsurgical clipping remains a widely adopted treatment; however, intraoperative rupture represents one of the most serious complications, significantly worsening surgical outcomes and patient prognosis [18, 19]. Rupture during clipping can intensify hemorrhage, trigger cerebral ischemia and neurological deficits, and increase postoperative mortality. Thus, precise identification of high-risk factors is essential for improving surgical safety and reducing complications.

Our study identified several independent risk factors for intraoperative rupture during IA clipping, including cerebral vasospasm, aneurysm size, morphology, anterior communicating artery location, preoperative Hunt-Hess grade, and the use of adjunctive techniques. These can be broadly categorized into anatomical and clinical determinants, each exerting distinct effects on surgical outcomes.

Aneurysm size and morphology emerged as key predictors. Larger aneurysms (≥10 mm) are more vulnerable to rupture due to thinner vessel walls and higher intraluminal pressure.

Table 2. Comparison of risk factor characteristics between training and validation groups

Variable	Training Group (n=188)	Validation Group (n=98)	External validation group (n=91)	Statistic Value	*P*-value
Rupture				0.32	0.852
Yes	38 (20.21%)	18 (18.37%)	16 (17.58%)		
No	150 (79.79%)	80 (81.63%)	75 (82.42%)		
Cerebral Vasospasm				0.486	0.784
Yes	70 (37.23%)	35 (35.71%)	30 (32.97%)		
No	118 (62.77%)	63 (64.29%)	61 (67.03%)		
Maximum Aneurysm Diameter				0.417	0.812
≥10 mm	72 (38.30%)	40 (40.82%)	33 (36.26%)		
<10 mm	116 (61.70%)	58 (59.18%)	58 (63.74%)		
Regular Morphology				1.388	0.499
Yes	92 (48.94%)	50 (51.02%)	39 (42.86%)		
No	96 (51.06%)	48 (48.98%)	52 (57.14%)		
Anterior Communicating Artery Aneurysm				0.994	0.608
Yes	53 (28.19%)	30 (30.61%)	22 (24.18%)		
No	135 (71.81%)	68 (69.39%)	69 (75.82%)		
Preoperative Hunt-Hess Grade				0.02	0.99
>III	83 (44.15%)	44 (44.90%)	40 (43.96%)		
≤III	105 (55.85%)	54 (55.10%)	51 (56.04%)		
Use of Adjunctive Techniques				0.749	0.688
Yes	41 (21.81%)	22 (22.45%)	24 (26.37%)		
No	147 (78.19%)	76 (77.55%)	67 (73.63%)		

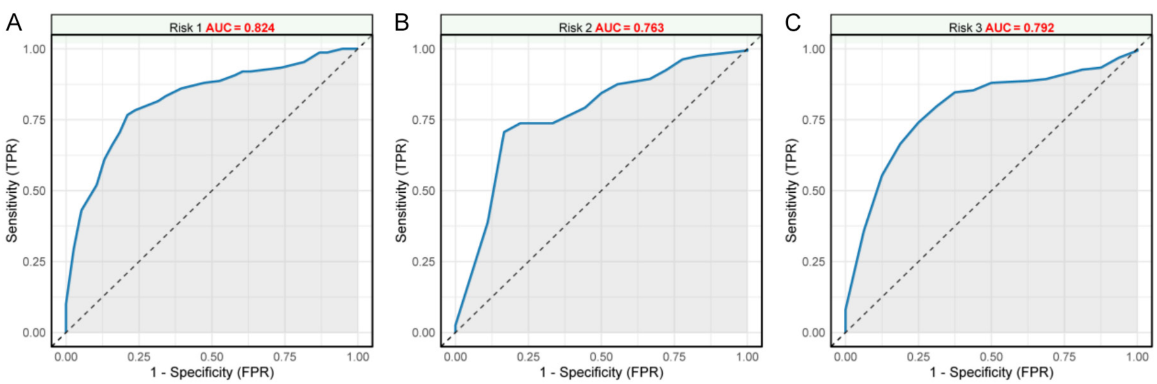

Figure 5. ROC curve analysis of the training and validation groups. A. ROC curve for the training group, AUC=0.824. B. ROC curve for the validation group, AUC=0.763. C. ROC curve for the external validation group, AUC=0.792. Note: ROC, Receiver Operating Characteristic; AUC, Area Under the Curve.

Sharma et al. [15] and Świątnicki et al. [20] similarly reported that increasing aneurysm dimensions are associated with higher rupture risk, likely due to impaired wall integrity and hemodynamic stress. Morphology also influences rupture propensity. Irregularly shaped aneurysms generally require more complex manipulation, elevating the risk of rupture, whereas regular aneurysms are technically easier to clip with fewer complications [21, 22]. Careful preoperative evaluation of aneurysm dimensions and morphology is therefore essential to guide individualized surgical strategies.

Aneurysms located at the anterior communicating artery carry higher rupture risk because of their complex anatomical positioning within critical cerebrovascular networks. Studies by Celikoglu et al. [22] and Mooney et al. [23] emphasized the value of detailed imaging to evalu-

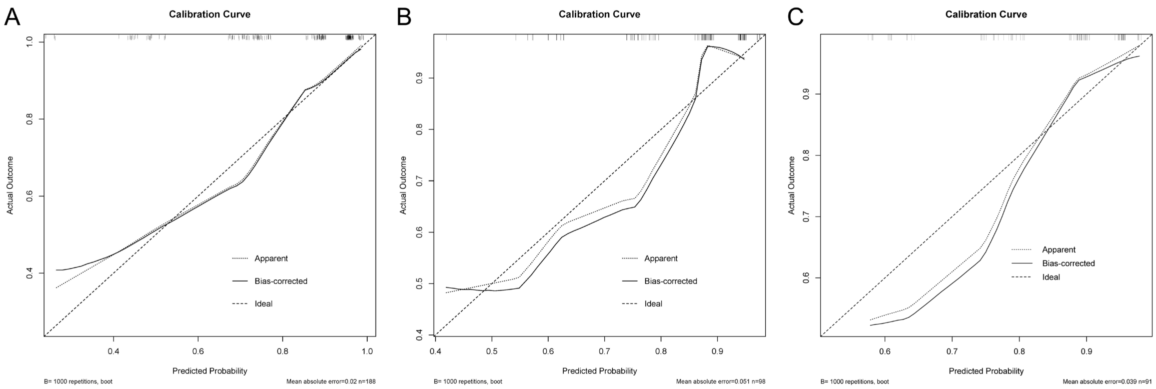

Figure 6. Calibration curve analysis of the training and validation groups. A. Calibration curve is for the training group. B. Calibration curve for the validation group. C. Calibration curve for the external validation group.

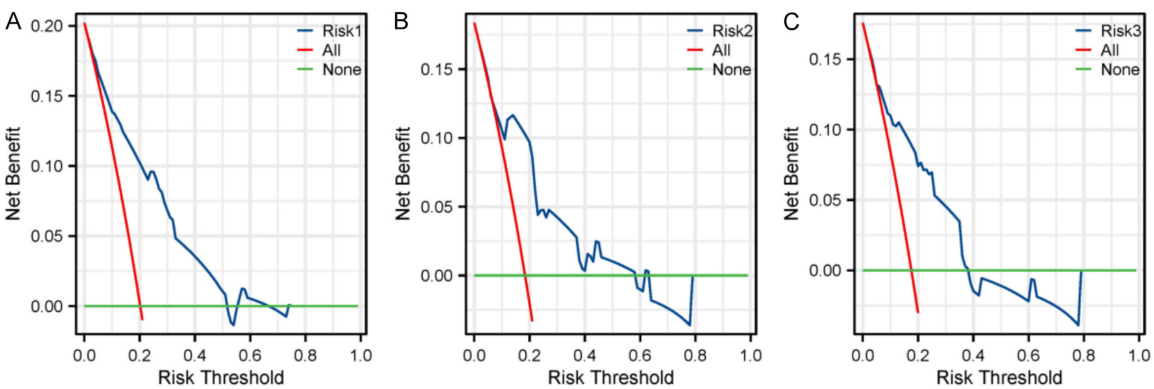

Figure 7. DCA analysis of the training and validation groups. A. The DCA curve of the training group. B. The DCA curve for the validation group. C. The DCA curve for the external validation group. Note: DCA, Decision Curve Analysis.

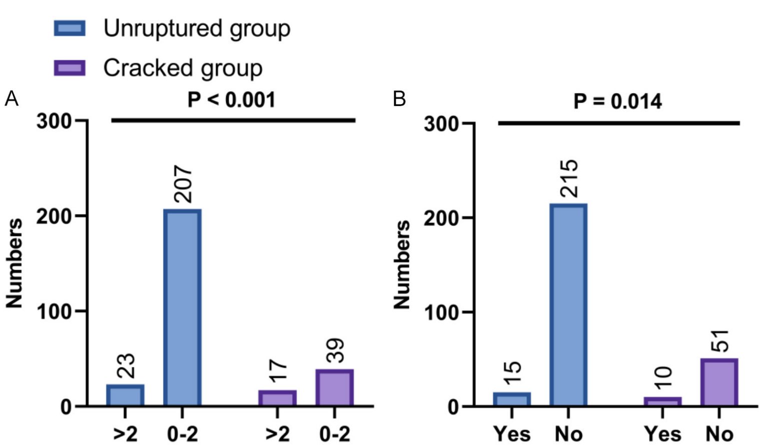

Figure 8. Six-month postoperative outcomes and complication incidence. A. mRS scores at six months postoperatively. B. Incidence of postoperative complications in patients. Note: mRS, Modified Rankin Scale.

ate aneurysm location, size, and adjacent vascular architecture for surgical planning. Moreover, Mistry et al. [24] suggested that partial endovascular coil embolization prior to clipping may reduce intraoperative rupture risk, although this approach was not examined in our study.

Clinical determinants such as cerebral vasospasm and preoperative Hunt-Hess grade also strongly influence rupture risk. Bordoni et al. [25] and Sharma et al. [19] reported that vasospasm increases rup-ture risk by causing vasoconstriction and disturbed blood flow, which heighten wall stress. Careful monitoring and timely management of vasospasm are therefore critical, especially in patients with prior SAH. Patients with preoperative Hunt-Hess grades >III are particularly vulnerable, as their unstable cerebrovascular status predisposes them to hemodynamic disturbances and surgical complications. Reports have shown that a higher Hunt-Hess grade is associated with worse postoperative outcomes [15], supporting its application in surgical risk stratification. In addition, Han et al. [26] identified hypertension, aneurysm neck dimensions, and irregular morphology as contributors to rupture risk, further supporting our findings.

By integrating both anatomical and clinical determinants, a more comprehensive understanding of intraoperative rupture risk can be achieved, thereby facilitating more accurate surgical planning and improved patient outcomes.

Although adjunctive techniques such as intraoperative blood flow imaging and advanced microscopy are designed to enhance surgical precision, our study identified their use as an independent risk factor for intraoperative rupture. This paradoxical finding may be explained by several mechanisms. First, these techniques are typically applied in technically demanding cases that inherently carry higher rupture risk, thus creating a confounding association. Second, reliance on adjunctive methods may prolong operative time and increase aneurysm manipulation, potentially elevating rupture risk despite improved visualization [15]. These findings suggest that adjunctive techniques, while valuable, should be employed judiciously, with careful consideration of case complexity and surgeon expertise.

Based on multivariate logistic regression, we developed a nomogram incorporating the identified risk factors to quantify intraoperative rupture risk. Validation using ROC analysis showed good discriminative ability, with AUCs of 0.824 in the training cohort and 0.763 in the validation cohort. Calibration curves demonstrated satisfactory agreement between predicted and observed outcomes, and DCA confirmed significant net clinical benefits across a risk threshold range of 0-78%. Together, these findings indicate that the model provides stable predictive accuracy and generalizability, supporting its application in clinical decision-making.

Intraoperative rupture was associated with significantly worse postoperative prognosis. Patients experiencing rupture exhibited higher six-month mRS scores, reflecting impaired functional recovery, and had higher complication rates, including infection, thrombosis, and multiple organ dysfunction. Frączek et al. [27] demonstrated that rupture risk is closely associated with aneurysm size and thrombus formation, consistent with our observation that larger aneurysms carry increased rupture risk. Yamagami et al. [28] further reported that aneurysms located in regions such as the basilar artery are often linked to poorer long-term outcomes, highlighting the importance of anatomical factors.

The nomogram model offers substantial clinical utility by enabling risk assessment at different stages of aneurysm management. Preoperatively, it facilitates identification of high-risk features such as large aneurysm size and cerebral vasospasm, thereby guiding individualized treatment strategies. For example, in patients with giant aneurysms, more cautious surgical manipulation or alternative approaches may be warranted to mitigate rupture risk. The model also emphasizes the need to balance technological support with surgical expertise, as excessive reliance on adjunctive techniques may fail to account for individual patient differences and result in suboptimal outcomes.

However, this study has several limitations. First, as a retrospective single-region analysis, the potential for selection bias and incomplete data may limit the generalizability of our findings. Second, although the model demonstrated satisfactory predictive ability, larger prospective multicenter studies are required to confirm its stability across diverse populations. Finally, as surgical and imaging technologies continue to advance, the predictive model may require refinement. Incorporating high-resolution imaging modalities and machine learning algorithms could further enhance risk stratification accuracy in future studies.

In conclusion, the proposed nomogram provides a reliable tool for predicting intraoperative rupture during microsurgical clipping of IA. By enabling personalized risk assessment, it supports optimized preoperative planning and may improve surgical outcomes, particularly in patients at high risk.

Disclosure of conflict of interest

None.

Address correspondence to: Jingku Ma, Department of Neuro Intensive Care Unit, No. 215 Hospital of Shaanxi Nuclear Industry, No. 52 Weiyang West Road, Qindu District, Xianyang 712000, Shaanxi, China. E-mail: majingku2013@163.com

References

[1] Li J, Tan Z, Yi X, Fu Y, Zhu L, Zeng F, Han Z, Ren Z, Zhang Y and Chen BT. Association of brain morphology and phenotypic profile in patients with unruptured intracranial aneurysm. Front Aging Neurosci 2023; 15: 1202699.

[2] Liu J, Cao F, Zhenmei N, Guo Y, Li Y, Yuan D, Jiang W and Yan J. Flow-diverter stents in intracranial aneurysm treatment: impact on covered cerebral artery branches. Int J Surg 2024; 110: 53-65.

[3] Kane SF, Butler E and Sindelar BD. Nontraumatic subarachnoid hemorrhage and ruptured intracranial aneurysm: recognition and evaluation. Am Fam Physician 2023; 108: 386-395.

[4] He Q, Wang W, Xiong Y, Tao C, Ma L and You C. Causal association between circulating inflammatory cytokines and intracranial aneurysm and subarachnoid hemorrhage. Eur J Neurol 2024; 31: e16326.

[5] D'Amato SA and Chang TR. Advances in intracranial hemorrhage: subarachnoid hemorrhage and intracerebral hemorrhage. Crit Care Clin 2023; 39: 71-85.

[6] Okamura K, Izumo T, Takahira R, Morofuji Y and Matsuo T. Detailed demonstration of the mechanism of acute subdural hematoma caused by ruptured intracranial aneurysm. Neurol India 2023; 71: 781-782.

[7] Tang H, Wang Q, Xu F, Zhang X, Zeng Z, Yan Y, Lu Z, Xue G, Zuo Q, Luo Y, Liu J and Huang Q. Underlying mechanism of hemodynamics and intracranial aneurysm. Chin Neurosurg J 2021; 7: 44.

[8] Liu S, Zhang P, Wu Y, Huang D, Yu M and Zhang M. Knowledge, attitude, practice and illness perception toward subarachnoid hemorrhage prevention and management among intracranial aneurysm patients. Clin Neurol Neurosurg 2024; 242: 108347.

[9] Han HJ, Kim JJ, Park KY, Park SK, Chung J and Kim YB. Subdural hygroma and hemorrhagic conversion after microsurgical clipping for unruptured intracranial aneurysm. Acta Neurochir (Wien) 2023; 165: 1251-1260.

[10] Zou L, Hou Y, Yu B, Li S and Du Y. The effect of intravascular interventional embolization and craniotomy on MMP-2, MMP-9 and caspase3 in serum of intracranial aneurysm patients. Exp Ther Med 2018; 16: 4511-4518.

[11] Vinacci G, Celentano A, Agosti E, Terrana AV, Vizzari FA, Nativo L, Baruzzi F, Tabano A, Locatelli D and Giorgianni A. Comaneci-assisted coiling of wide-necked intracranial aneurysm: a single-center preliminary experience. J Clin Med 2022; 11: 6650.

[12] Molyneux A, Kerr R, Stratton I, Sandercock P, Clarke M, Shrimpton J and Holman R. International Subarachnoid Aneurysm Trial (ISAT) of neurosurgical clipping versus endovascular coiling in 2143 patients with ruptured intracranial aneurysms: a randomised trial. Lancet 2002; 360: 1267-1274.

[13] Inci S and Karakaya D. The nightmare of aneurysm surgery: intraoperative rupture. World Neurosurg 2023; 180: 70.

[14] Qian W, Chen Y, Zhu Q, Chen A and Lan Q. Microsurgical clipping of multiple intracranial aneurysms via the keyhole approach. World Neurosurg 2024; 187: e282-e288.

[15] Sharma GR, Joshi S, Paudel P, Shah DB, Karki P, Basnet A and Evans G. Risk factors and outcome analysis of patients with intraoperative rupture (IOR) of ruptured cerebral aneurysm during microsurgical clipping. Br J Neurosurg 2024; 38: 1086-1090.

[16] He Q, You C and Cheng Y. Letter: The Ruptured Arteriovenous Malformation Grading Scale (RAGS): an extension of the hunt and hess scale to predict clinical outcome for patients with ruptured brain arteriovenous malformations. Neurosurgery 2020; 87: E725.

[17] Cruddas L and Baker DM. Does Modified Rankin Score (mRS) matter? The impact of stroke severity on carotid artery endarterectomy (CEA) outcomes. Ann Vasc Surg 2023; 93: 351-354.

[18] Yin Z, Zhang Q, Zhao Y, Lu J, Ge P, Xie H, Wu D, Yu S, Kang S, Zhang Q, Zhang Y, Zhang D, Zhao J and Liu X. Prevalence and procedural risk of intracranial atherosclerotic stenosis coexisting with unruptured intracranial aneurysm. Stroke 2023; 54: 1484-1493.

[19] Seong J, Kim J, Lee S and Kim B. Two consecutive ruptured intracranial aneurysm in patient with multiple intracranial aneurysms. J Cerebrovasc Endovasc Neurosurg 2024; 26: 174-180.

[20] Świątnicki W, Szymański J, Szymańska A and Komuński P. Predictors of intraoperative aneurysm rupture, aneurysm remnant, and brain ischemia following microsurgical clipping of intracranial aneurysms: single-center, retrospective cohort study. J Neurol Surg A Cent Eur Neurosurg 2021; 82: 410-416.

[21] Goertz L, Hamisch C, Telentschak S, Kabbasch C, von Spreckelsen N, Stavrinou P, Timmer M, Goldbrunner R, Brinker G and Krischek B. Impact of aneurysm shape on intraoperative rupture during clipping of ruptured intracranial aneurysms. World Neurosurg 2018; 118: e806-e812.

[22] Celikoglu E, Eksi MS, Bastaci F, Hazneci J, Borekci A, Topal A, Selahi O, Berikol G, Koromer RA and Hakan T. Risk factors for intracranial aneurysm rupture: a clinical case series and systematic review of the literature. Turk Neurosurg 2024; 34: 624-639.

[23] Mooney MA, Brigeman S, Bohl MA, Simon ED, Sheehy JP, Chang SW and Spetzler RF. Analysis of overlapping surgery in patients undergoing microsurgical aneurysm clipping: acute and long-term outcomes from the barrow ruptured aneurysm trial. J Neurosurg 2018; 129: 711-717.

[24] Mistry AM, Naidugari J, Meyer KS, Chen CJ, Williams BJ, Morton RP, Abecassis IJ and Ding D. Partial coil embolization before surgical clipping of ruptured intracranial aneurysms. Acta Neurochir (Wien) 2024; 166: 293.

[25] Bordoni L, Nasuti C, Fedeli D, Galeazzi R, Laudadio E, Massaccesi L, López-Rodas G and Gabbianelli R. Early impairment of epigenetic pattern in neurodegeneration: additional mechanisms behind pyrethroid toxicity. Exp Gerontol 2019; 124: 110629.

[26] Han J, Pan H, Yao L, Jin E, Pan W and Xiong L. Comparison of microsurgical clipping with intravascular interventional embolization in the treatment of ruptured aneurysms and risk factors for intraoperative rupture and bleeding. Am J Transl Res 2023; 15: 3451-3459.

[27] Frączek MJ, Błoński MJ, Kliś KM, Krzyżewski RM, Polak J, Stachura K and Kwinta BM. Predictors of intraoperative intracranial aneurysm rupture in patients with subarachnoid hemorrhage: a retrospective analysis. Acta Neurol Belg 2023; 123: 1717-1724.

[28] Yamagami K, Hatano T, Nakahara I, Ishii A, Ando M, Chihara H, Ogura T, Suzuki K, Kondo D, Kamata T, Higashi E, Sakai S, Sakamoto H, Iihara K and Nagata I. Long-term outcomes after intraprocedural aneurysm rupture during coil embolization of unruptured intracranial aneurysms. World Neurosurg 2020; 134: e289-e297.

Table S1. Predictor VIF and multicollinearity assessment

Variable	VIF	Interpretation
Age	1.064	Low multicollinearity
Vascular Narrowing	1.013	Low multicollinearity
Vasospasm	1.032	Low multicollinearity
Maximum Aneurysm Diameter	1.012	Low multicollinearity
Irregular Shape	1.049	Low multicollinearity
Anterior Communicating Aneurysm	1.044	Low multicollinearity
Preoperative Hunt-Hess Grading	1.024	Low multicollinearity
Auxiliary Technique Usage	1.037	Low multicollinearity

Note: VIF, variance inflation factor.